

AN ADAPTIVE FINITE ELEMENT METHOD FOR THE LAPLACE–BELTRAMI OPERATOR ON IMPLICITLY DEFINED SURFACES*

ALAN DEMLOW[†] AND GERHARD DZIUK[‡]

Abstract. We present an adaptive finite element method for approximating solutions to the Laplace–Beltrami equation on surfaces in \mathbb{R}^3 which may be implicitly represented as level sets of smooth functions. Residual-type a posteriori error bounds which show that the error may be split into a “residual part” and a “geometric part” are established. In addition, implementation issues are discussed and several computational examples are given.

Key words. Laplace–Beltrami operator, adaptive finite element methods, a posteriori error estimation, boundary value problems on surfaces

AMS subject classifications. 58J32, 65N15, 65N30

DOI. 10.1137/050642873

1. Introduction. In this paper we derive residual-based a posteriori error estimates for piecewise linear finite element approximations to solutions of the Laplace–Beltrami equation

$$(1.1.1) \quad \begin{aligned} -\Delta_\Gamma u &= f \text{ on } \Gamma, \\ u &= 0 \text{ on } \partial\Gamma. \end{aligned}$$

Here Γ is a connected two-dimensional surface embedded in \mathbb{R}^3 , and $-\Delta_\Gamma$ is the Laplace–Beltrami operator on Γ . $\partial\Gamma$ is required to be “piecewise curvilinear” in a sense which we will make precise below. We also allow $\partial\Gamma = \emptyset$, in which case the conditions $\int_\Gamma f \, d\sigma = \int_\Gamma u \, d\sigma = 0$ are required to guarantee existence and uniqueness of u . Here $d\sigma$ is the surface measure on Γ .

A finite element method for (1.1.1) was introduced in [Dz88]. Let Γ_h be a polyhedral approximation to Γ having triangular faces, and let S_h be the continuous functions which are affine on each face of Γ_h . We then let $u_h \in S_h$ solve

$$(1.1.2) \quad \int_{\Gamma_h} \nabla_{\Gamma_h} u_h \nabla_{\Gamma_h} v_h \, d\sigma_h = \int_{\Gamma_h} v_h f_h \, d\sigma_h \quad \forall v_h \in S_h.$$

Here ∇_{Γ_h} is the tangential derivative on Γ_h , σ_h is the surface measure on Γ_h , and f_h is an approximation to f on Γ_h . As above, we require the side conditions $\int_{\Gamma_h} f_h \, d\sigma_h = \int_{\Gamma_h} u_h \, d\sigma_h = 0$ if $\partial\Gamma_h = \emptyset$.

A key feature of our theoretical development is that Γ is represented as the 0 level set of a signed distance function d with $|d(x)| = \text{dist}(x, \Gamma)$. Our approach requires

*Received by the editors October 17, 2005; accepted for publication (in revised form) July 14, 2006; published electronically February 15, 2007. This research is based upon work partially supported by a National Science Foundation postdoctoral research fellowship and a grant of the Deutsche Forschungsgemeinschaft.

<http://www.siam.org/journals/sinum/45-1/64287.html>

[†]Department of Mathematics, University of Kentucky, Patterson Office Tower 715, Lexington, KY 40506-0027 (demlow@ms.uky.edu).

[‡]Abteilung für Angewandte Mathematik, Hermann-Herder-Str. 10, 79104 Freiburg, Germany (gerd@mathematik.uni-freiburg.de).

access to the derivatives of d (the normal vector and curvature tensor) and also requires that Γ_h lie in a strip about Γ on which a unique orthogonal projection $a(x)$ onto Γ is defined. This projection is instrumental in suitably defining the discrete data f_h and also in carrying out both a priori and a posteriori error analysis. Also, if $\partial\Gamma$ is nonempty we shall require that $\partial\Gamma = a(\partial\Gamma_h)$ so that $\partial\Gamma$ is in a sense piecewise curvilinear. This is similar to requiring polygonal boundaries when performing finite element calculations on domains in \mathbb{R}^n in that it rules out “variational crimes” resulting from boundary approximations.

In practice, Γ often is defined as a level set of a function ζ which is not a distance function. In this situation one must approximate the projection $a(x)$ numerically, and the other necessary geometric information may then be computed in a straightforward fashion. In practical terms, the resulting finite element code requires the user to supply the data f , the level set function ζ and its first and second derivatives, and an initial mesh which lies in a sufficiently narrow strip about Γ to guarantee that the projection a is a bijection between Γ_h and Γ . In what follows we shall discuss some details of our implementation in addition to providing a posteriori error estimates.

Optimal-order $H^1(\Gamma)$ and $L_2(\Gamma)$ a priori estimates for the method (1.1.2) were proved in [Dz88]. Roughly speaking, the finite element error may be broken into an *almost-best-approximation* term typical of finite element methods in \mathbb{R}^n , a *geometric error term* which is due to the discretization of Γ , and a *data approximation term* due to the approximation of f on Γ by f_h on Γ_h . On a mesh whose elements have diameter h , the latter two terms are of order h^2 for typical choices of f_h and are thus of higher order when the error is measured in the H^1 -norm.

In this paper we provide a posteriori error control in the $H^1(\Gamma)$ -norm via residual-type estimators. As in the a priori analysis, the error is split into three terms: a *residual indicator term*, a *geometric error term*, and a *data approximation term*. Computation of these error terms requires pointwise access to geometric information, in particular to the projection a and the normal vector and curvature tensor on Γ . However, the asymptotically dominant term requires no explicit geometric quantities except those which are necessary to compute the discrete data f_h .

A relatively simple setting is assumed here in order to concentrate on effects arising from the discretization of Γ . In particular, we do not consider problems with nonconstant coefficients, the case where $a(\Gamma_h) \neq \Gamma$, lower-order terms, or nonhomogeneous Dirichlet or Neumann boundary conditions. These additional complexities may be handled in much the same way as for problems on polygonal domains in \mathbb{R}^2 , so we refer, for example, to the works [DR98], [DW00], [BCD04], [MN05], and [AO00], where many of these issues are considered. Under suitable assumptions, our development also holds largely unchanged for surfaces of codimension 1 which are immersed in \mathbb{R}^n , $n \geq 2$.

In order to conclude the introduction, we briefly describe other strategies for performing adaptive finite element calculations on surfaces. One possibility is the use of a global parametrization to represent Γ and define a suitable mesh. This approach was taken in [AP05] to perform adaptive finite element calculations on the sphere. The key to this method is a global parametrization which maps a triangulated planar domain onto the sphere in such a way that the resulting curved “triangles” are isotropic (shape-regular). A more general approach using local parametrizations (charts) to represent 2- and 3-manifolds is described in [Ho01].

The technique we present here has several advantages when compared with the two described above. Extending the use of global parametrizations to surfaces other than the sphere is relatively difficult because a new parametrization must be found for

every surface on which computations are to be performed. In addition, the analysis of the Clément-type interpolant used to prove reliability of a posteriori estimates in [AP05] is specific to the sphere and would have to be redone for other surfaces. In contrast, implementation of our method is quite straightforward for the sphere and may be carried out in a fairly general way for a large class of surfaces. The analysis we give here also is not restricted to any particular surface. The use of local parametrizations described in [Ho01] provides a framework for computations on manifolds which is in some ways more general than that which we propose here. However, the use of overlapping local charts adds to the complexity of both the resulting finite element code and the theoretical analysis. Indeed, the issue of approximation theory when using local charts is not addressed rigorously in [Ho01]. A final advantage of our approach is that it provides rigorous theoretical background for adaptive methods in certain situations in which no parametrization is available, such as implicit computations of surfaces evolving, for example, by mean curvature flow (cf. [Dz91], [BMN05], [CDDRR04]).

This paper is organized as follows: In section 2 we give a number of preliminaries and assumptions necessary for our theoretical development. In section 3 we then prove global a posteriori upper bounds and local lower bounds. In section 4 our implementation is described. In section 5, we demonstrate the flexibility of our approach by describing computational experiments on three different surfaces: a spherical subdomain with a nonempty boundary, a torus (which is nonconvex and has a topological type different than that of the sphere), and an ellipsoid (which requires numerical approximation of the distance function).

2. Preliminaries and assumptions.

2.1. The continuous surface Γ . We assume that Γ is a connected C^2 compact hypersurface which is the zero level set of a signed distance function $|d(x)| = \text{dist}(x, \Gamma)$ defined on an open subset U_0 of \mathbb{R}^3 . If $\partial\Gamma = \emptyset$ we also assume for simplicity that $d < 0$ on the interior of Γ and $d > 0$ on the exterior. $\vec{\nu} = \nabla d$ is then the outward-pointing unit normal on Γ . Note that $|\vec{\nu}| = 1$ wherever d is defined. Let also $\mathbf{H} : \mathbb{R}^3 \rightarrow \mathbb{R}^{3 \times 3}$ be the Weingarten map defined by

$$(2.2.1) \quad \mathbf{H}_{ij}(x) = \vec{\nu}_{i,x_j}(x) = \vec{\nu}_{j,x_i}(x),$$

that is, $\mathbf{H}(x) = D^2 d(x)$, and let $\kappa_i(x)$, $i = 1, 2$, and 0 be the eigenvalues of $\mathbf{H}(x)$. For $x \in \Gamma$, κ_1 and κ_2 are the principal curvatures.

Next we define the projection

$$(2.2.2) \quad a(x) = x - d(x)\vec{\nu}(x).$$

We then let $U \subset \mathbb{R}^3$ be a strip of width δ about Γ , where $\delta > 0$ is sufficiently small to ensure that the decomposition

$$(2.2.3) \quad x = a(x) + d(x)\vec{\nu}(x)$$

is unique for $x \in U$. We require that

$$(2.2.4) \quad \delta < \left[\max_{i=1,2} \|\kappa_i\|_{L_\infty(\Gamma)} \right]^{-1}.$$

For $x \in U$, we also note the useful formula

$$(2.2.5) \quad \kappa_i(x) = \frac{\kappa_i(a(x))}{1 + d(x)\kappa_i(a(x))}$$

for the curvature of parallel surfaces, cf. Lemma 14.17 of [GT98].

The condition (2.2.4) is sufficient to ensure that the decomposition (2.2.3) is *locally* unique (cf. [GT98, section 14.6]), but we require that it be globally unique. This global requirement is a simplifying assumption which restricts our presentation to embedded surfaces. Immersed surfaces (including surfaces with self-intersections) could also be considered with slight changes to our presentation.

We may uniquely extend a function ψ defined on Γ to U by

$$(2.2.6) \quad \psi^\ell(x) = \psi(a(x))$$

for $x \in U$. Let

$$(2.2.7) \quad \mathbf{P} = \mathbf{I} - \vec{\nu} \otimes \vec{\nu},$$

where \otimes is the tensor or outer product $\vec{a} \otimes \vec{b} = \vec{a} \vec{b}^T$ (vectors here are in column form). We then define the tangential gradient

$$(2.2.8) \quad \nabla_\Gamma \psi = \nabla \psi^\ell - (\vec{\nu} \cdot \nabla \psi^\ell) \vec{\nu} = \mathbf{P} \nabla \psi^\ell$$

for ψ defined on Γ and extended to U via (2.2.6). Note that $\nabla_\Gamma \psi$ depends only on the values of ψ on Γ even though its definition formally involves the extension of ψ to Γ . Note also that $-\Delta_\Gamma = -\nabla_\Gamma \cdot \nabla_\Gamma$. Finally, we denote by $H^1(\Gamma)$ the functions on Γ having a tangential gradient in $L^2(\Gamma)$.

2.2. The discrete surface Γ_h and mesh \mathcal{T}_h . Let $\Gamma_h \subset U$ be a polyhedron consisting of a set \mathcal{T}_h of triangular faces, that is, $\Gamma_h = \cup_{T \in \mathcal{T}_h} \overline{T}$. Let also $\vec{\nu}_h$ denote the (piecewise constant) unit outer normal on Γ_h , and let \mathcal{N} denote the set of nodes of triangles in \mathcal{T}_h . We assume that $a : \Gamma_h \rightarrow \Gamma$ is bijective and that $\vec{\nu} \cdot \vec{\nu}_h > 0$ everywhere on Γ_h . We note that it is often simplest to define Γ_h so that $\mathcal{N} \subset \Gamma$, but this is not theoretically required in any way. Also denote by h_T the diameter of $T \in \mathcal{T}_h$. Given $z \in \mathcal{N}$, we define the patch $\omega_z = \text{interior}(\cup_{\overline{T} \ni z} \overline{T})$ and let $h_z = \max_{T \subset \omega_z} h_T$. Also, let \mathcal{E} denote the set of edges of triangles in \mathcal{T}_h . Finally, $\varphi_z \in S_h$ denotes the canonical basis function associated to z , that is, $\varphi_{z_i}(z_j) = \delta_{ij}$ for $z_i, z_j \in \mathcal{N}$.

Analyses of a posteriori estimates for finite element methods on domains in \mathbb{R}^n typically assume that the underlying mesh is shape-regular, that is, all elements in \mathcal{T}_h have a bounded aspect ratio. Under this assumption, constants depending on the aspect ratio of the elements of the mesh are then bounded and may be absorbed into a global constant of moderate size. This approach is reasonable because typical mesh refinement algorithms preserve shape-regularity.

The situation is somewhat more complicated in the current context of finite element methods on surfaces. The first issue which arises is that the mesh is perturbed after each refinement by projecting newly created nodes onto the continuous surface Γ via a . While these perturbations are asymptotically negligible, we are not aware of a proof that the refinement/perturbation procedure described here maintains shape regularity beginning from an arbitrary shape-regular mesh with nodes on Γ and lying in U . A second problem is that, in contrast to the situation in \mathbb{R}^n , shape regularity does not automatically imply that the number of triangles sharing a given node is bounded. However, if the number of elements in the patches of the initial coarse mesh used to begin the refinement algorithm is bounded, we may guarantee that such a bound will hold for all subsequent meshes by applying a suitable refinement algorithm. This is, in particular, the case for the newest-node subdivision algorithm.

As we have not been able to theoretically guarantee that a family of meshes maintains shape regularity under mesh refinement, we take the following approach.

We first prove a posteriori bounds which do not assume shape regularity. In these estimates, lack of shape regularity is penalized by a single factor. In our computational examples we do not include this penalty factor in our estimator but instead monitor it to ensure that mesh quality remains acceptable. In our examples, the penalty term remains of moderate size when refining meshes which initially lie within U .

2.3. Lifts and extensions of functions. Given a function v_h defined on Γ_h , we define the lift \tilde{v}_h by $v_h(x) = \tilde{v}_h(a(x))$ for $x \in \Gamma_h$. We may then extend \tilde{v}_h to U by (2.2.6). For v_h defined on Γ_h and $x \in U$, we thus define

$$(2.2.9) \quad v_h^\ell(x) = \tilde{v}_h(a(x)).$$

The overall effect of (2.2.9) is to extend v_h defined on Γ_h to U . Formally, however, this operation consists of a lift to Γ followed by extension to U . We emphasize that *all* extensions of functions to U referred to in this paper are constant along normals to Γ . Thus for our purposes extensions of functions defined on Γ and of functions defined on Γ_h have essentially the same properties.

Letting $\vec{\nu}_h$ denote the normal on Γ_h , we define for $x \in \Gamma_h$

$$(2.2.10) \quad \mathbf{P}_h(x) = \mathbf{I} - \vec{\nu}_h(x) \otimes \vec{\nu}_h(x)$$

so that, for V defined on U and $x \in \Gamma_h$,

$$(2.2.11) \quad \nabla_{\Gamma_h} V(x) = \mathbf{P}_h \nabla V(x).$$

We see from (2.2.2) and (2.2.9) that, for $x \in \Gamma_h$ and v_h defined on Γ_h ,

$$(2.2.12) \quad \nabla v_h^\ell(x) = [(\mathbf{P} - d\mathbf{H})(x)] \nabla v_h^\ell(a(x)).$$

Since $\vec{\nu} \cdot \vec{\nu} \equiv 1$, we have $\vec{\nu}\mathbf{H} = \mathbf{H}\vec{\nu} = 0$ and $\mathbf{P}\mathbf{H} = \mathbf{H}\mathbf{P} = \mathbf{H}$ so that, for $x \in \Gamma_h$,

$$(2.2.13) \quad \nabla v_h^\ell(x) = [(\mathbf{I} - d\mathbf{H})(x)][\mathbf{P}(x)] \nabla v_h^\ell(a(x)) = [(\mathbf{I} - d\mathbf{H})(x)] \nabla_{\Gamma} v_h^\ell(a(x)).$$

Thus

$$(2.2.14) \quad \nabla_{\Gamma_h} v_h(x) = \nabla_{\Gamma_h} v_h^\ell(x) = [\mathbf{P}_h(x)][(\mathbf{I} - d\mathbf{H})(x)][\mathbf{P}(x)] \nabla_{\Gamma} v_h^\ell(a(x)).$$

Correspondingly, for $\psi \in H^1(\Gamma)$ (2.2.6) yields

$$(2.2.15) \quad \nabla_{\Gamma_h} \psi^\ell(x) = [\mathbf{P}_h(x)][(\mathbf{I} - d\mathbf{H})(x)][\mathbf{P}(x)] \nabla_{\Gamma} \psi(a(x)).$$

For $x \in \Gamma_h$, (2.2.13) yields

$$(2.2.16) \quad \nabla_{\Gamma} v_h^\ell(a(x)) = [(\mathbf{I} - d\mathbf{H})(x)]^{-1} \nabla v_h^\ell(x).$$

The invertibility of $[(\mathbf{I} - d\mathbf{H})(x)]$ on U may be derived from (2.2.4) and (2.2.5). Indeed, if e_1 and e_2 are the eigenvectors of \mathbf{H} corresponding to $\kappa_1(x)$ and $\kappa_2(x)$, then $[(\mathbf{I} - d\mathbf{H})(x)]^{-1} = \vec{\nu} \otimes \vec{\nu} + (1 + d(x)\kappa_1(a(x)))e_1 \otimes e_1 + (1 + d(x)\kappa_2(a(x)))e_2 \otimes e_2$. We shall need to compute $\nabla_{\Gamma} v_h^\ell$ when $v_h \in S_h$. In such cases we initially have access only to the tangential derivative $\nabla_{\Gamma_h} v_h$ and not to ∇v_h^ℓ , which according to (2.2.16) is necessary to compute $\nabla_{\Gamma} v_h^\ell$. Since $\nabla_{\Gamma_h} v_h(x) = [\mathbf{P}_h(x)] \nabla v_h^\ell(x)$, we have $0 = \nabla v_h^\ell(x) \cdot \vec{\nu} = \nabla_{\Gamma_h} v_h(x) \cdot \vec{\nu} + (\vec{\nu}_h \cdot \vec{\nu}) \nabla v_h^\ell(x) \cdot \vec{\nu}_h$. Thus

$$(2.2.17) \quad \nabla v_h^\ell(x) \cdot \vec{\nu}_h = - \frac{\nabla_{\Gamma_h} v_h(x) \cdot \vec{\nu}}{\vec{\nu}_h \cdot \vec{\nu}},$$

and for $x \in \Gamma_h$

$$(2.2.18) \quad \nabla v_h^\ell(x) = \left[\mathbf{I} - \frac{\vec{\nu}_h \otimes \vec{\nu}}{\vec{\nu}_h \cdot \vec{\nu}} \right] \nabla_{\Gamma_h} v_h(x).$$

Combining (2.2.16) and (2.2.18), we thus find that, for $x \in \Gamma_h$,

$$(2.2.19) \quad \nabla_{\Gamma} v_h^\ell(a(x)) = [(\mathbf{I} - d\mathbf{H})(x)]^{-1} \left[\mathbf{I} - \frac{\vec{\nu}_h \otimes \vec{\nu}}{\vec{\nu}_h \cdot \vec{\nu}} \right] \nabla_{\Gamma_h} v_h(x).$$

Next we state an integral equality which we shall use repeatedly. For $x \in \Gamma_h$, let

$$(2.2.20) \quad \mu_h(x) \, d\sigma_h(x) = d\sigma(a(x)),$$

and also let

$$(2.2.21) \quad \mathbf{A}_h(x) = \mathbf{A}_h^\ell(a(x)) = \frac{1}{\mu_h(x)} [\mathbf{P}(x)][(\mathbf{I} - d\mathbf{H})(x)][\mathbf{P}_h(x)][(\mathbf{I} - d\mathbf{H})(x)][\mathbf{P}(x)].$$

Then from (2.2.14) and (2.2.15), we have

$$(2.2.22) \quad \int_{\Gamma_h} \nabla_{\Gamma_h} v_h \nabla_{\Gamma_h} \psi_h \, d\sigma_h = \int_{\Gamma} \mathbf{A}_h^\ell \nabla_{\Gamma} v_h^\ell \nabla_{\Gamma} \psi_h^\ell \, d\sigma.$$

Note that this equality holds without regard to the original domain of definition of v_h and ψ ; that is, we may for example replace ψ_h and ψ_h^ℓ with ψ^ℓ and ψ , respectively, where $\psi \in H^1(\Gamma)$. We also emphasize that the quantities d and \mathbf{H} in (2.2.21) are always evaluated on the discrete surface Γ_h , even though \mathbf{A}_h^ℓ often appears in integrals over the continuous surface Γ .

Finally we give an explicit formula for the quantity μ_h defined above. The proof of this formula is tedious but elementary, and we sketch it in Appendix A.

PROPOSITION 2.1. *Assume that $x \in \Gamma_h$. Then*

$$(2.2.23) \quad \mu_h(x) = (1 - d(x)\kappa_1(x))(1 - d(x)\kappa_2(x))\vec{\nu} \cdot \vec{\nu}_h.$$

2.4. Interpolation and Poincaré inequality. In this section we define an interpolant and prove error bounds for it. Given $\psi \in L_1(\Gamma)$ and $z \in \mathcal{N}$, we let

$$(2.2.24) \quad \psi_z^\ell = \frac{1}{\int_{\omega_z} \varphi_z \, d\sigma_h} \int_{\omega_z} \varphi_z \psi^\ell \, d\sigma_h$$

and define

$$(2.2.25) \quad I_h \psi^\ell = \sum_{z \in \mathcal{N}} \psi_z^\ell \varphi_z.$$

A similar interpolant is used, for example, in [FV06] to prove a posteriori bounds on a domain in \mathbb{R}^2 . Noting that $\{\varphi_z\}_{z \in \mathcal{N}}$ is a partition of unity, we then have the following relationship:

$$(2.2.26) \quad \int_{\Gamma_h} (\psi^\ell - I_h \psi^\ell) \, d\sigma_h = \sum_{z \in \mathcal{N}} \int_{\omega_z} (\psi^\ell - \psi_z^\ell) \varphi_z \, d\sigma_h = 0.$$

LEMMA 2.2 (Poincaré inequality). Let $\psi \in H^1(\Gamma)$. Let m_z be the number of elements sharing the node z , and let $\tilde{\omega}_z$ be the lift of the patch ω_z onto Γ . Then for each $z \in \mathcal{N}$,

$$(2.2.27) \quad \|\psi^\ell - \psi_z^\ell\|_{L_2(\omega_z)} \leq C \max_{T \subset \omega_z} \sqrt{|T|} m_z \max_{T \subset \omega_z} \frac{h_T}{\sqrt{|T|}} \|\mathbf{A}_h\|_{\ell_2, L_\infty(\omega_z)}^{\frac{1}{2}} \|\nabla_\Gamma \psi\|_{L_2(\tilde{\omega}_z)}.$$

Let also $z \in \bar{e} \in \mathcal{E}$. Then

$$(2.2.28) \quad \|\psi^\ell - \psi_z^\ell\|_{L_2(e)} \leq C \sqrt{|e|} m_z \max_{T \subset \omega_z} \frac{h_T}{\sqrt{|T|}} \|\mathbf{A}_h\|_{\ell_2, L_\infty(\omega_z)}^{\frac{1}{2}} \|\nabla_\Gamma \psi\|_{L_2(\tilde{\omega}_z)}.$$

Here $\|\mathbf{A}_h\|_{\ell_2, L_\infty(\omega_z)} = \|\|\mathbf{A}_h\|_{\ell_2 \rightarrow \ell_2}\|_{L_\infty(\omega_z)}$, where $\|\cdot\|_{\ell_2 \rightarrow \ell_2}$ is the standard matrix 2-norm, and C does not depend on any essential quantities.

Remark 2.3. The terms in (2.2.27) and (2.2.28) may be classified as follows: In shape-regular meshes the quantities $\max_{T \subset \omega_z} \sqrt{|T|}$ and $\sqrt{|e|}$ may be reduced to h_z and $h_z^{1/2}$, respectively, where h_z is the maximum element diameter in ω_z . The factor m_z accounts for the number of elements sharing the vertex z if this number is not known to be bounded, and the factor $\max_{T \subset \omega_z} h_T / \sqrt{|T|}$ accounts for the aspect ratio of T . If \mathcal{T}_h is shape-regular and m_z is bounded, we thus have

$$(2.2.29) \quad \|\psi^\ell - \psi_z^\ell\|_{L_2(\omega_z)} \leq C h_z \|\mathbf{A}_h\|_{\ell_2, L_\infty(\omega_z)}^{\frac{1}{2}} \|\nabla_{\Gamma_h} \psi^\ell\|_{L_2(\omega_z)},$$

$$(2.2.30) \quad \|\psi^\ell - \psi_z^\ell\|_{L_2(e)} \leq C h_z^{\frac{1}{2}} \|\mathbf{A}_h\|_{\ell_2, L_\infty(\omega_z)}^{\frac{1}{2}} \|\nabla_\Gamma \psi\|_{L_2(\tilde{\omega}_z)},$$

where C does not depend on essential quantities.

Proof. We first show that I_h is locally L_2 -stable independent of mesh properties. Note first that

$$(2.2.31) \quad \|\psi_z^\ell\|_{L_2(\omega_z)} = |\omega_z|^{1/2} |\psi_z^\ell| \leq |\omega_z|^{1/2} \frac{\|\varphi_z\|_{L_2(\omega_z)}}{\|\varphi_z\|_{L_1(\omega_z)}} \|\psi^\ell\|_{L_2(\omega_z)}.$$

If z is an interior node, we let $\hat{\omega}_z$ be a regular m_z -gon with vertices lying on the unit circle. If z is a boundary node, then we let $\hat{\omega}_z$ be one half of a regular $2m_z$ -gon with vertices lying on the unit circle. In either case the reference domain $\hat{\omega}_z$ is convex and may be broken into m_z congruent triangles with the origin being a vertex of each. There is a natural piecewise-affine transformation $F_z : \hat{\omega}_z \rightarrow \omega_z$. We denote by \hat{T} the inverse image of $T \subset \omega_z$ and by \hat{u} the inverse image of $u \in H^1(\Gamma_h)$ under this transformation. For $p = 1$ or $p = 2$ and any $\hat{T} \subset \hat{\omega}_z$,

$$(2.2.32) \quad \|\varphi_z\|_{L_p(\omega_z)}^p = \sum_{T \subset \omega_z} \int_T \varphi_z^p d\sigma_h = \sum_{T \subset \omega_z} \frac{|T|}{|\hat{T}|} \int_{\hat{T}} \hat{\varphi}_z^p d\hat{x} = |\omega_z| \frac{\int_{\hat{T}} \hat{\varphi}_z^p d\hat{x}}{|\hat{T}|}.$$

An elementary calculation yields $\sqrt{|T|} \frac{\|\hat{\varphi}_z\|_{L_2(\hat{T})}}{\|\hat{\varphi}_z\|_{L_1(\hat{T})}} = \sqrt{\frac{3}{2}}$, which when combined with (2.2.31) and (2.2.32) yields

$$(2.2.33) \quad \|\psi_z^\ell\|_{L_2(\omega_z)} \leq \sqrt{\frac{3}{2}} \|\psi^\ell\|_{L_2(\omega_z)}.$$

Thus for any $K \in \mathbb{R}$,

$$(2.2.34) \quad \|\psi^\ell - \psi_z^\ell\|_{L_2(\omega_z)} \leq \left(1 + \sqrt{\frac{3}{2}}\right) \|\psi^\ell - K\|_{L_2(\omega_z)}.$$

Choosing $K = \frac{1}{|\hat{\omega}_z|} \int_{\hat{\omega}_z} \hat{\psi}^\ell d\hat{x}$ and noting that $\nabla \hat{\psi}^\ell = \nabla_{\Gamma_h} \psi^\ell \nabla F_z$, we next find that

$$\begin{aligned}
 \|\psi^\ell - K\|_{L_2(\omega_z)}^2 &= \sum_{T \subset \omega_z} \frac{|T|}{|\hat{T}|} \int_{\hat{T}} (\hat{\psi}^\ell - K)^2 d\hat{x} \\
 &= \frac{1}{|\hat{T}|} \max_{T \subset \omega_z} |T| \int_{\hat{\omega}_z} (\hat{\psi}^\ell - K)^2 d\hat{x} \\
 (2.2.35) \quad &\leq C_P(\hat{\omega}_z)^2 \frac{1}{|\hat{T}|} \max_{T \subset \omega_z} |T| \int_{\hat{\omega}_z} |\nabla \hat{\psi}^\ell|^2 d\hat{x} \\
 &= C_P(\hat{\omega}_z)^2 \frac{1}{|\hat{T}|} \max_{T \subset \omega_z} |T| \sum_{T \subset \omega_z} \frac{|\hat{T}|}{|T|} \int_T |\nabla_{\Gamma_h} \psi^\ell \nabla F_z|^2 d\sigma_h \\
 &\leq C_P(\hat{\omega}_z)^2 \max_{T \subset \omega_z} |T| \max_{T \subset \omega_z} \frac{\|\nabla F_z|_T\|_{\ell_2 \rightarrow \ell_2}^2}{|T|} \|\nabla_{\Gamma_h} \psi^\ell\|_{L_2(\omega_z)}^2.
 \end{aligned}$$

Here C_P is the Poincaré constant for $\hat{\omega}_z$. It is not hard to compute that

$$(2.2.36) \quad \|\nabla F_z|_T\|_{\ell_2 \rightarrow \ell_2} \leq C m_z h_T,$$

where C does not depend on any essential quantities. Combining (2.2.34), (2.2.35), and (2.2.36) and finally applying (2.2.22) yields (2.2.27).

The proof of (2.2.28) is accomplished by employing a trace inequality and slightly modifying the preceding proof. Assume that $e \subset \bar{T} \subset \bar{\omega}_z$. Let \tilde{T} be the unit simplex in \mathbb{R}^2 (note that this is not the same as the reference element employed above), with \hat{e} denoting the transformation of e to \tilde{T} . Letting \hat{F}_T denote the affine transformation of \tilde{T} to T , we note that $\|\hat{F}_T\|_{\ell_2 \rightarrow \ell_2} \leq h_T$. Employing a trace inequality on \tilde{T} then yields

$$\begin{aligned}
 \|\psi^\ell - \psi_z^\ell\|_{L_2(e)} &\leq \sqrt{|e|} \|\hat{\psi}^\ell - \psi_z^\ell\|_{L_2(\hat{e})} \\
 (2.2.37) \quad &\leq C \sqrt{|e|} (\|\hat{\psi}^\ell - \psi_z^\ell\|_{L_2(\tilde{T})} + \|\nabla \hat{\psi}^\ell\|_{L_2(\tilde{T})}) \\
 &\leq C \sqrt{\frac{|e|}{|T|}} (\|\psi^\ell - \psi_z^\ell\|_{L_2(T)} + h_T \|\nabla_{\Gamma_h} \psi^\ell\|_{L_2(T)}).
 \end{aligned}$$

$\sqrt{|e|/|T|} h_T \|\nabla_{\Gamma_h} \psi^\ell\|_{L_2(T)}$ is clearly bounded by the right-hand side of (2.2.28), so we must consider only the first term in the last line above.

Letting \hat{T} , $\hat{\omega}_z$, and K be as defined as before, we first proceed as in (2.2.35) to find that

$$\begin{aligned}
 \sqrt{\frac{|e|}{|T|}} \|\psi^\ell - K\|_{L_2(T)} &\leq \sqrt{\frac{|e|}{|\hat{T}|}} \|\hat{\psi}^\ell - K\|_{L_2(\hat{T})} \\
 (2.2.38) \quad &\leq \sqrt{\frac{|e|}{|\hat{T}|}} \|\hat{\psi}^\ell - K\|_{L_2(\hat{\omega}_z)} \\
 &\leq C \sqrt{|e|} m_z \max_{T \subset \omega_z} \frac{h_T}{\sqrt{|T|}} \|\nabla_{\Gamma_h} \psi^\ell\|_{L_2(\omega_z)}.
 \end{aligned}$$

Proceeding as in (2.2.31) through (2.2.34), we next find that

$$\begin{aligned}
 (2.2.39) \quad \sqrt{\frac{|e|}{|T|}} \|(\psi^\ell - K)_z\|_{L_2(T)} &\leq \sqrt{|e|} \|(\psi^\ell - K)_z\| \\
 &\leq \sqrt{\frac{3}{2}} \sqrt{\frac{|e|}{|\omega_z|}} \|\psi^\ell - K\|_{L_2(\omega_z)}.
 \end{aligned}$$

Combining (2.2.39) and (2.2.35) yields

$$\begin{aligned}
 \sqrt{\frac{|e|}{|T|}} \|(\psi^\ell - K)_z\|_{L_2(T)} &\leq C\sqrt{|e|} \max_{T \subset \omega_z} \sqrt{\frac{|T|}{|\omega_z|}} m_z \max_{T \subset \omega_z} \frac{h_T}{\sqrt{|T|}} \|\nabla_{\Gamma_h} \psi^\ell\|_{L_2(\omega_z)} \\
 (2.2.40) \qquad \qquad \qquad &\leq C\sqrt{|e|} m_z \max_{T \subset \omega_z} \frac{h_T}{\sqrt{|T|}} \|\nabla_{\Gamma_h} \psi^\ell\|_{L_2(\omega_z)}.
 \end{aligned}$$

Since $\|\psi^\ell - \psi_z^\ell\|_{L_2(T)} \leq \|\psi^\ell - K\|_{L_2(T)} + \|(\psi^\ell - K)_z\|_{L_2(T)}$, combining (2.2.37), (2.2.38), and (2.2.40) with (2.2.22) completes the proof of (2.2.28). \square

3. The estimator. In this section we develop a computable and reliable estimator for $\|\nabla_\Gamma(u - u_h^\ell)\|_{L_2(\Gamma)}$.

3.1. Residual equation. We first derive a residual equation. Let $\psi \in H_0^1(\Gamma)$, where $H_0^1(\Gamma)$ is the set of functions in $H^1(\Gamma)$ having a vanishing trace if $\partial\Gamma \neq \emptyset$ and having a vanishing mean value if $\partial\Gamma = \emptyset$. Following [Dz88] and applying (2.2.22), we find that, for $\psi \in H^1(\Gamma)$ and $\psi_h \in S_h$,

$$\begin{aligned}
 \int_\Gamma \nabla_\Gamma(u - u_h^\ell) \nabla_\Gamma \psi \, d\sigma &= \int_{\Gamma_h} f^\ell \mu_h \psi^\ell \, d\sigma_h - \int_\Gamma [\mathbf{P} - \mathbf{A}_h^\ell] \nabla_\Gamma u_h^\ell \nabla_\Gamma \psi \, d\sigma \\
 (3.3.1) \qquad \qquad \qquad &\quad - \int_{\Gamma_h} \nabla_{\Gamma_h} u_h \nabla_{\Gamma_h} \psi^\ell \, d\sigma_h
 \end{aligned}$$

and

$$\begin{aligned}
 \int_\Gamma \nabla_\Gamma(u - u_h^\ell) \nabla_\Gamma \psi_h^\ell \, d\sigma &= \int_{\Gamma_h} f^\ell \mu_h \psi_h \, d\sigma_h - \int_\Gamma [\mathbf{P} - \mathbf{A}_h^\ell] \nabla_\Gamma u_h^\ell \nabla_\Gamma \psi_h^\ell \, d\sigma \\
 &\quad - \int_{\Gamma_h} \nabla_{\Gamma_h} u_h \nabla_{\Gamma_h} \psi_h \, d\sigma_h \\
 (3.3.2) \qquad \qquad \qquad &= \int_{\Gamma_h} (f^\ell \mu_h - f_h) \psi_h \, d\sigma_h - \int_\Gamma [\mathbf{P} - \mathbf{A}_h^\ell] \nabla_\Gamma u_h^\ell \nabla_\Gamma \psi_h^\ell \, d\sigma.
 \end{aligned}$$

Combining (3.3.1) and (3.3.2), we find that

$$\begin{aligned}
 \int_\Gamma \nabla_\Gamma(u - u_h^\ell) \nabla_\Gamma \psi \, d\sigma &= \int_\Gamma \nabla_\Gamma(u - u_h^\ell) \nabla_\Gamma \psi \, d\sigma - \int_\Gamma \nabla_\Gamma(u - u_h^\ell) \nabla_\Gamma \psi_h^\ell \, d\sigma \\
 &\quad + \int_\Gamma \nabla_\Gamma(u - u_h^\ell) \nabla_\Gamma \psi_h^\ell \, d\sigma \\
 (3.3.3) \qquad \qquad \qquad &= \int_{\Gamma_h} f^\ell \mu_h (\psi^\ell - \psi_h) \, d\sigma_h - \int_{\Gamma_h} \nabla_{\Gamma_h} u_h \nabla_{\Gamma_h} (\psi^\ell - \psi_h) \, d\sigma_h \\
 &\quad - \int_\Gamma [\mathbf{P} - \mathbf{A}_h^\ell] \nabla_\Gamma u_h^\ell \nabla_\Gamma \psi \, d\sigma + \int_{\Gamma_h} (f^\ell \mu_h - f_h) \psi_h \, d\sigma_h.
 \end{aligned}$$

Next we note that

$$\begin{aligned}
 (3.3.4) \quad & - \int_{\Gamma_h} \nabla_{\Gamma_h} u_h \nabla_{\Gamma_h} (\psi^\ell - \psi_h) \, d\sigma_h \\
 &= \sum_{T \in \mathcal{T}_h} \int_T \Delta_{\Gamma_h} u_h (\psi^\ell - \psi_h) \, d\sigma_h - \int_{\partial T} \nabla_{\Gamma_h} u_h \cdot \vec{n} (\psi^\ell - \psi_h) \, ds \\
 &= \int_{\Gamma_h} \Delta_{\Gamma_h} u_h (\psi^\ell - \psi_h) \, d\sigma_h - \frac{1}{2} \sum_{T \in \mathcal{T}} \int_{\partial T} [[\nabla_{\Gamma_h} u_h]] (\psi^\ell - \psi_h) \, ds,
 \end{aligned}$$

where $\Delta_{\Gamma_h} u_h$ is a piecewise polynomial and \vec{n} is the conormal vector to the triangle T (that is, $\vec{n} \cdot \vec{\nu}_h = 0$). In the current situation $\Delta_{\Gamma_h} u_h$ is identically 0, but we include it to make clear how the corresponding term would appear in other situations. Also, let e be an edge shared by elements T_1 and T_2 which have normals \vec{n}_1 and \vec{n}_2 , respectively. Then $[[\nabla_{\Gamma_h} u_h]] = \nabla_{\Gamma_h} u_h|_{T_1} \cdot \vec{n}_1 - \nabla_{\Gamma_h} u_h|_{T_2} \cdot \vec{n}_2$ is the jump in the normal derivative across e . If $e \subset \partial\Gamma_h$ we set $[[\nabla_{\Gamma_h} u_h]]|_e = 0$. Note that \vec{n}_1 lies in the plane of T_1 and \vec{n}_2 lies in the plane of T_2 , so in contrast to the situation which arises on domains in \mathbb{R}^n , we generally have $\vec{n}_1 \neq -\vec{n}_2$. Finally, we insert (3.3.4) into (3.3.3) to find

$$\begin{aligned}
 (3.3.5) \quad & \int_{\Gamma} \nabla_{\Gamma} (u - u_h^\ell) \nabla_{\Gamma} \psi \, d\sigma = \int_{\Gamma_h} (f^\ell \mu_h + \Delta_{\Gamma_h} u_h) (\psi^\ell - \psi_h) \, d\sigma_h \\
 & - \frac{1}{2} \sum_{T \in \mathcal{T}} \int_{\partial T} [[\nabla_{\Gamma_h} u_h]] (\psi^\ell - \psi_h) \, ds - \int_{\Gamma} [\mathbf{P} - \mathbf{A}_h^\ell] \nabla_{\Gamma} u_h^\ell \nabla_{\Gamma} \psi \, d\sigma \\
 & + \int_{\Gamma_h} (f^\ell \mu_h - f_h) \psi_h \, d\sigma_h \\
 & \equiv \text{I} + \text{II} + \text{III} + \text{IV}.
 \end{aligned}$$

3.2. A posteriori upper bound (reliability). We begin by bounding term I of (3.3.5). Let $\psi_h = I_h \psi^\ell$, and let $s_z = m_z \max_{T \subset \omega_z} h_T / \sqrt{|T|}$. Also let $R = f^\ell \mu_h + \Delta_{\Gamma_h} u_h$, and let $\{R_z\}_{z \in \mathcal{N}}$ be constants. Recalling that $\{\varphi_z\}_{z \in \mathcal{N}}$ is a partition of unity, recalling (2.2.25) and (2.2.26), and applying Lemma 2.2, we then have

$$\begin{aligned}
 (3.3.6) \quad \text{I} &= \sum_{z \in \mathcal{N}} \int_{\omega_z} R (\psi^\ell - \psi_z^\ell) \varphi_z \, d\sigma_h = \sum_{z \in \mathcal{N}} \int_{\omega_z} (R - R_z) (\psi^\ell - \psi_z^\ell) \varphi_z \, d\sigma_h \\
 &\leq C \sum_{z \in \mathcal{N}} \max_{T \subset \omega_z} \sqrt{|T|} s_z \|\mathbf{A}_h\|_{\ell_2, L_\infty(\omega_z)}^{\frac{1}{2}} \cdot \|\varphi_z (R - R_z)\|_{L_2(\omega_z)} h_z \|\nabla_{\Gamma} \psi\|_{L_2(\tilde{\omega}_z)}.
 \end{aligned}$$

Next we turn to bounding the term II. Applying Lemma 2.2, we find

$$\begin{aligned}
 (3.3.7) \quad \text{II} &= -\frac{1}{2} \sum_{z \in \mathcal{N}} \sum_{\bar{e} \ni z} \int_e \varphi_z [[\nabla_{\Gamma_h} u_h]] (\psi^\ell - \psi_z^\ell) \, ds \\
 &\leq C \sum_{z \in \mathcal{N}} \sum_{\bar{e} \ni z} \sqrt{|e|} s_z \|\mathbf{A}_h\|_{\ell_2, L_\infty(\omega_z)}^{\frac{1}{2}} \|\varphi_z [[\nabla_{\Gamma_h} u_h]]\|_{L_2(e)} \|\nabla_{\Gamma} \psi\|_{L_2(\tilde{\omega}_z)}.
 \end{aligned}$$

Let

$$(3.3.8) \quad \eta_z = s_z \left(\max_{T \subset \omega_z} \sqrt{|T|} \|\varphi_z (R - R_z)\|_{L_2(\omega_z)} + \sum_{\bar{e} \ni z} \sqrt{|e|} \|\varphi_z [[\nabla_{\Gamma_h} u_h]]\|_{L_2(e)} \right).$$

Combining (3.3.6) and (3.3.7) and noting that each element T has only three nodes, we thus find that

$$\begin{aligned}
 \text{I} + \text{II} &\leq C \sum_{z \in \mathcal{N}} \|\mathbf{A}_h\|_{\ell_2, L_\infty(\omega_z)}^{\frac{1}{2}} \eta_z \|\nabla_\Gamma \psi\|_{L_2(\tilde{\omega}_z)} \\
 (3.3.9) \quad &\leq C \left(\sum_{z \in \mathcal{N}} \|\mathbf{A}_h\|_{\ell_2, L_\infty(\omega_z)} \eta_z^2 \right)^{\frac{1}{2}} \left(\sum_{z \in \mathcal{N}} \|\nabla_\Gamma \psi\|_{L_2(\tilde{\omega}_z)}^2 \right)^{\frac{1}{2}} \\
 &\leq C \left(\sum_{z \in \mathcal{N}} \|\mathbf{A}_h\|_{\ell_2, L_\infty(\omega_z)} \eta_z^2 \right)^{\frac{1}{2}} \|\nabla_\Gamma \psi\|_{L_2(\Gamma)},
 \end{aligned}$$

where C does not depend on \mathcal{T}_h or any other essential quantities.

In order to bound the term III, we use (2.2.19) to compute

$$\begin{aligned}
 \text{III} &= - \sum_{z \in \mathcal{N}} \int_{\tilde{\omega}_z} \varphi_z^\ell [\mathbf{P} - \mathbf{A}_h^\ell] \nabla_\Gamma u_h^\ell \nabla_\Gamma \psi \, d\sigma \\
 (3.3.10) \quad &\leq \sum_{z \in \mathcal{N}} \left\| \sqrt{\varphi_z^\ell} [\mathbf{P} - \mathbf{A}_h^\ell] \nabla_\Gamma u_h^\ell \right\|_{L_2(\tilde{\omega}_z)} \left\| \sqrt{\varphi_z^\ell} \nabla_\Gamma \psi \right\|_{L_2(\tilde{\omega}_z)} \\
 &= \sum_{z \in \mathcal{N}} \left\| \sqrt{\mu_h} \sqrt{\varphi_z} [\mathbf{P} - \mathbf{A}_h] [\mathbf{I} - d\mathbf{H}]^{-1} \left[\mathbf{I} - \frac{\vec{\nu}_h \otimes \vec{\nu}}{\vec{\nu}_h \cdot \vec{\nu}} \right] \nabla_{\Gamma_h} u_h \right\|_{L_2(\omega_z)} \\
 &\quad \cdot \left\| \sqrt{\varphi_z^\ell} \nabla_\Gamma \psi \right\|_{L_2(\tilde{\omega}_z)}.
 \end{aligned}$$

Defining

$$(3.3.11) \quad \mathbf{B}_h = \sqrt{\mu_h} [\mathbf{P} - \mathbf{A}_h] [\mathbf{I} - d\mathbf{H}]^{-1} \left[\mathbf{I} - \frac{\vec{\nu}_h \otimes \vec{\nu}}{\vec{\nu}_h \cdot \vec{\nu}} \right]$$

and recalling that $\sum_{z \in \mathcal{N}} \varphi_z = \sum_{z \in \mathcal{N}} \varphi_z^\ell \equiv 1$, we finally compute

$$\begin{aligned}
 \text{III} &\leq \left(\sum_{z \in \mathcal{N}} \|\sqrt{\varphi_z} \mathbf{B}_h \nabla_{\Gamma_h} u_h\|_{L_2(\omega_z)}^2 \right)^{1/2} \left(\sum_{z \in \mathcal{N}} \|\sqrt{\varphi_z^\ell} \nabla_\Gamma \psi\|_{L_2(\tilde{\omega}_z)}^2 \right)^{1/2} \\
 (3.3.12) \quad &= \|\mathbf{B}_h \nabla_{\Gamma_h} u_h\|_{L_2(\Gamma_h)} \|\nabla_\Gamma \psi\|_{L_2(\Gamma)}.
 \end{aligned}$$

Finally we bound the term IV. First we note that, for $z \in \mathcal{N}$ and with ψ_z^ℓ defined as in (2.2.24),

$$\begin{aligned}
 (3.3.13) \quad \|\sqrt{\varphi_z} \psi_z^\ell\|_{L_2(\Omega_z)} &= \sqrt{\int_{\omega_z} \varphi_z \, d\sigma_h} \frac{1}{\int_{\omega_z} \varphi_z \, d\sigma_h} \left| \int_{\omega_z} \varphi_z \psi_z^\ell \, d\sigma_h \right| \\
 &\leq \|\sqrt{\varphi_z} \psi^\ell\|_{L_2(\omega_z)}.
 \end{aligned}$$

Since $\psi \in H_0^1(\Gamma)$ has either a vanishing trace on $\partial\Omega$ or a vanishing mean value over

Ω , we may apply (3.3.13) and a Poincaré inequality to compute

$$\begin{aligned}
 \text{IV} &= \int_{\Gamma_h} (f^\ell \mu_h - f_h) \psi_h \, d\sigma_h \\
 &= \sum_{z \in \mathcal{N}} \int_{\omega_z} (f^\ell \mu_h - f_h) \varphi_z \psi_z^\ell \, d\sigma_h \\
 &\leq \sum_{z \in \mathcal{N}} \|\sqrt{\varphi_z}(f^\ell \mu_h - f_h)\|_{L_2(\omega_z)} \|\sqrt{\varphi_z} \psi_z^\ell\|_{L_2(\omega_z)} \\
 &\leq \sum_{z \in \mathcal{N}} \|\sqrt{\varphi_z}(f^\ell \mu_h - f_h)\|_{L_2(\omega_z)} \|\sqrt{\varphi_z} \psi^\ell\|_{L_2(\omega_z)} \\
 (3.3.14) \quad &\leq \sum_{z \in \mathcal{N}} \left\| \frac{1}{\sqrt{\mu_h}} \right\|_{L_\infty(\omega_z)} \|\sqrt{\varphi_z}(f^\ell \mu_h - f_h)\|_{L_2(\Gamma_h)} \left\| \sqrt{\varphi_z} \psi^\ell \right\|_{L_2(\bar{\omega}_z)} \\
 &\leq \left(\sum_{z \in \mathcal{N}} \left\| \frac{1}{\mu_h} \right\|_{L_\infty(\omega_z)} \|\sqrt{\varphi_z}(f^\ell \mu_h - f_h)\|_{L_2(\Gamma_h)}^2 \right)^{1/2} \|\psi\|_{L_2(\Gamma)} \\
 &\leq C_P(\Gamma) \left(\sum_{z \in \mathcal{N}} \left\| \frac{1}{\mu_h} \right\|_{L_\infty(\omega_z)} \|\sqrt{\varphi_z}(f^\ell \mu_h - f_h)\|_{L_2(\Gamma_h)}^2 \right)^{1/2} \|\nabla_\Gamma \psi\|_{L_2(\Gamma)}.
 \end{aligned}$$

Making the substitution $\psi = u - u_h^\ell$ if $\partial\Gamma \neq \emptyset$ or $\psi = u - u_h^\ell - \frac{1}{|\Gamma|} \int_\Gamma (u - u_h^\ell) \, d\sigma$ if $\partial\Gamma = \emptyset$ while combining (3.3.3), (3.3.12), and (3.3.14) yields

$$\begin{aligned}
 \|\nabla_\Gamma(u - u_h^\ell)\|_{L_2(\Gamma)}^2 &\leq \left[C \left(\sum_{z \in \mathcal{N}} \|\mathbf{A}_h\|_{\ell_2, L_\infty(\omega_z)} \eta_z^2 \right)^{1/2} + \|\mathbf{B}_h \nabla_{\Gamma_h} u_h\|_{L_2(\Gamma_h)} \right. \\
 (3.3.15) \quad &\quad \left. + C_P(\Gamma) \left(\sum_{z \in \mathcal{N}} \left\| \frac{1}{\mu_h} \right\|_{L_\infty(\omega_z)} \|\sqrt{\varphi_z}(f^\ell \mu_h - f_h)\|_{L_2(\Gamma_h)}^2 \right)^{1/2} \right] \\
 &\quad \cdot \|\nabla_\Gamma(u - u_h^\ell)\|_{L_2(\Gamma)}.
 \end{aligned}$$

Dividing (3.3.15) through by $\|\nabla_\Gamma(u - u_h^\ell)\|_{L_2(\Gamma)}$ then yields the following theorem.

THEOREM 3.1. *Under the assumptions in section 2,*

$$(3.3.16) \quad \|\nabla_\Gamma(u - u_h^\ell)\|_{L_2(\Gamma)} \leq \mathcal{R} + \mathcal{G} + \mathcal{D},$$

where

$$(3.3.17) \quad \mathcal{R} = C \left(\sum_{z \in \mathcal{N}} \|\mathbf{A}_h\|_{\ell_2, L_\infty(\omega_z)} \eta_z^2 \right)^{1/2},$$

$$(3.3.18) \quad \mathcal{G} = \|\mathbf{B}_h \nabla_{\Gamma_h} u_h\|_{L_2(\Gamma_h)},$$

and

$$(3.3.19) \quad \mathcal{D} = C_P(\Gamma) \left(\sum_{z \in \mathcal{N}} \left\| \frac{1}{\mu_h} \right\|_{L_\infty(\omega_z)} \|\sqrt{\varphi_z}(f^\ell \mu_h - f_h)\|_{L_2(\Gamma_h)}^2 \right)^{1/2}.$$

Here $\eta_z = s_z(\max_{T \subset \omega_z} \sqrt{|T|} \|\varphi_z(R - R_z)\|_{L_2(\omega_z)} + \sum_{\bar{e} \ni z} \sqrt{|e|} \|\varphi_z[\nabla_{\Gamma_h} u_h]\|_{L_2(e)})$ as in (3.3.8), the constants R_z in η_z may be freely chosen, and C does not depend on T_h or Γ .

We make a few brief remarks concerning Theorem 3.1, beginning with the *residual term* \mathcal{R} . First we note that if the nodes of Γ_h lie on Γ , then $\|[(\mathbf{P} - \mathbf{A}_h)(x)]\|_{\ell_2 \rightarrow \ell_2} \leq Ch_T^2$ for $x \in T$ (cf. [Dz88]). Thus up to a higher-order term, \mathcal{R} is bounded by $C(\sum_{z \in \mathcal{N}} \eta_z^2)^{1/2}$. Next we consider the *geometric error term* \mathcal{G} . Note first that unlike the residual term \mathcal{R} , it contains no unknown constants. Secondly, \mathcal{G} is heuristically of higher order since $\|\mathbf{B}_h\|_{\ell_2 \rightarrow \ell_2} \leq C\|\mathbf{P} - \mathbf{A}_h\|_{\ell_2 \rightarrow \ell_2} \leq Ch_T^2$. The *data approximation term* \mathcal{D} is 0 if we let $f_h = \mu_h f^\ell$ and assume exact quadrature, both of which we shall do in our numerical tests. In [Dz88] the definition $f_h(x) = f^\ell(x) - \frac{1}{|\Gamma_h|} \int_{\Gamma_h} f^\ell d\sigma_h$ is made. This choice has the advantage of not requiring the computation of the ratio μ_h of the continuous to the discrete measure and still leads to optimal-order H^1 and L_2 estimates. However, computation of \mathcal{R} and \mathcal{G} requires access to μ_h in any case, so we shall use the definition $f_h = \mu_h f^\ell$ and thereby exclude \mathcal{D} . A final note concerning \mathcal{D} is that it includes the global Poincaré constant $C_P(\Gamma)$. In contrast to the terms \mathcal{R} and \mathcal{G} , \mathcal{D} is thus not entirely built up of quantities which are locally determined.

Finally, we note that the dominant term in (3.3.16) does not depend explicitly on geometric information about Γ . Since $\|\mathbf{A}_h - \mathbf{P}\|_{\ell_2, L_\infty(\omega_z)} \leq C(\tilde{\omega}_z)h_z^2$, we may compute $\mathcal{G} \leq (\sum_{z \in \mathcal{N}} C(\tilde{\omega}_z)h_z^4 \|\sqrt{\varphi_z} \nabla_{\Gamma_h} u_h\|_{L_2(\omega_z)}^2)^{1/2}$. Also, $\mathcal{R} \leq C(\sum_{z \in \mathcal{N}} \eta_z^2 + C(\Gamma)h_z^2 \eta_z^2)^{1/2}$. Finally, as shown in [Dz88], \mathcal{D} is of higher order even if the choice $f_h(x) = f^\ell(x) - \frac{1}{|\Gamma_h|} \int_{\Gamma_h} f^\ell d\sigma_h$ is made. Thus the dominant part of the a posteriori upper bound is $C(\sum_{z \in \mathcal{N}} \eta_z^2)^{1/2}$, exactly as for problems in planar domains.

The estimator given in Theorem 3.1 could in principle be implemented, but it is possible to define a more convenient estimator for practical use. Recalling the comments of section 2.2, we may simplify it by assuming shape-regularity. In addition, residual estimators are typically calculated elementwise instead of patchwise, so we define an alternate estimator which allows mostly elementwise calculations (the only exception is the term involving $\|A_h\|$, which must be patch-based). In our computations we shall apply the estimator naturally derived from the following corollary.

COROLLARY 3.2. *Assume that $f_h = \mu_h f^\ell$, that \mathcal{T}_h is shape-regular, and that m_z is bounded. Then*

(3.3.20)

$$\|\nabla_\Gamma(u - u_h)\|_{L_2(\Gamma)} \leq \sqrt{2} \left(\sum_{T \in \mathcal{T}_h} C \|\mathbf{A}_h\|_{\ell_2, L_\infty(\omega_T)} \eta_T^2 + \|\mathbf{B}_h \nabla_{\Gamma_h} u_h\|_{L_2(T)}^2 \right)^{1/2} \equiv \Theta.$$

Here $\omega_T = \cup_{z \in \bar{T}} \omega_z$, $\eta_T = h_T \|R\|_{L_2(T)} + h_T^{1/2} \|[\nabla_{\Gamma_h} u_h]\|_{L_2(\partial T)}$, and C depends on $\max_{z \in \mathcal{N}} m_z$ and the minimum angle over all elements of \mathcal{T}_h .

The proof of Corollary 3.2 follows by setting $R_z = 0$ in (3.3.8) and noting that, under the assumptions that \mathcal{T}_h is shape-regular and m_z is bounded, h_T is equivalent to h_z for all vertices z of T and to $|e|$ for all $e \subset \partial T$. \square

3.3. A posteriori lower bound (efficiency). In this section we prove a local a posteriori lower bound which is a counterpart to the upper bound in Corollary 3.2. Such lower bounds verify (up to higher-order terms) that the stated a posteriori estimate does not overestimate the actual error and also are an essential ingredient in proving the convergence of adaptive methods; cf. [MNS02].

PROPOSITION 3.3. Assume that $f_h = \mu_h f^\ell$, that \mathcal{T}_h is shape-regular, and that m_z is bounded. Then for $T \in \mathcal{T}_h$,

$$(3.3.21) \quad \eta_T \leq C \|\mathbf{A}_h\|_{\ell_2, L_\infty(\omega_T)}^{1/2} (\|\nabla_\Gamma(u - u_h^\ell)\|_{L_2(\omega_T)} + \|\mathbf{B}_h \nabla_{\Gamma_h} u_h\|_{L_2(\omega_T)}) \\ + Ch_T \|R - R_T\|_{L_2(\omega_T)}.$$

Here C depends on $\max_{z \in \mathcal{N}: z \in \bar{T}} m_z$ and the minimum angle of the elements in ω_T , and R_T is an arbitrary piecewise linear function.

Proof. We shall follow the well-known proof of Verfürth (cf. [Ver89]). First let $z \in \mathcal{N}$ and $T \subset \omega_z$. Letting z_i , $1 \leq i \leq 3$, be the nodes of T , we define the bubble function $\phi_T = \prod_{i=1}^3 \varphi_{z_i}$. In addition, let R_T be an arbitrary piecewise linear approximation to R on T . Let also \tilde{T} denote the natural lift of T to Γ . Then using (3.3.5) with $\psi = R_T \phi_T^\ell$ and $\psi_h = 0$ and noting that $\phi_T = 0$ on $\partial \tilde{T}$, we have

$$(3.3.22) \quad \int_T R R_T \phi_T \, d\sigma_h = \int_{\tilde{T}} \nabla_\Gamma(u - u_h^\ell) \nabla_\Gamma(R_T \phi_T^\ell) \, d\sigma \\ + \int_{\tilde{T}} [\mathbf{I} - \mathbf{A}_h^\ell] \nabla_\Gamma u_h^\ell \nabla_\Gamma(R_T \phi_T^\ell) \, d\sigma \\ \leq (\|\nabla_\Gamma(u - u_h^\ell)\|_{L_2(\tilde{T})} + \|[\mathbf{I} - \mathbf{A}_h^\ell] \nabla_\Gamma u_h^\ell\|_{L_2(\tilde{T})}) \|\nabla_\Gamma(R_T \phi_T^\ell)\|_{L_2(\tilde{T})} \\ \leq (\|\nabla_\Gamma(u - u_h^\ell)\|_{L_2(\tilde{T})} + \|\mathbf{B}_h \nabla_{\Gamma_h} u_h\|_{L_2(T)}) \\ \cdot \|\mathbf{A}_h\|_{L_\infty(T)}^{1/2} \|\nabla_{\Gamma_h}(R_T \phi_T)\|_{L_2(T)}.$$

Since $R_T \phi_T$ is a polynomial, we may apply an inverse inequality to find

$$(3.3.23) \quad \|\nabla_{\Gamma_h}(R_T \phi_T)\|_{L_2(T)} \leq Ch_T^{-1} \|R_T \phi_T\|_{L_2(T)} \leq Ch_T^{-1} \|R_T\|_{L_2(T)},$$

where C depends only on the shape-regularity of T . Thus

$$(3.3.24) \quad \int_T R R_T \phi_T \, d\sigma_h \\ \leq Ch_T^{-1} \|\mathbf{A}_h\|_{L_\infty(T)}^{1/2} (\|\nabla_\Gamma(u - u_h^\ell)\|_{L_2(\tilde{T})} + \|\mathbf{B}_h \nabla_{\Gamma_h} u_h\|_{L_2(T)}) \|R_T\|_{L_2(T)}.$$

Applying Theorem 2.2 of [AO00], we next note that

$$(3.3.25) \quad \|R_T\|_{L_2(T)}^2 \leq \|\sqrt{\phi_T} R_T\|_{L_2(T)}^2 \\ \leq \left(\|\sqrt{\phi_T}(R - R_T)\|_{L_2(T)} + \left(\int_T R R_T \phi_T \, d\sigma_h \right)^{1/2} \right) \|R_T\|_{L_2(T)}.$$

Combining the previous inequalities, we thus find

$$(3.3.26) \quad \|R_T\|_{L_2(T)}^2 \leq C [\|R - R_T\|_{L_2(T)} + h_T^{-1} \|\mathbf{A}_h\|_{L_\infty(T)}^{1/2} (\|\nabla_\Gamma(u - u_h^\ell)\|_{L_2(\tilde{T})} \\ + \|\mathbf{B}_h \nabla_{\Gamma_h} u_h\|_{L_2(T)})] \|R_T\|_{L_2(T)}.$$

Thus

$$(3.3.27) \quad h_T \|R\|_{L_2(T)} \leq C [\|\mathbf{A}_h\|_{L_\infty(T)}^{1/2} (\|\nabla_\Gamma(u - u_h^\ell)\|_{L_2(\tilde{T})} + \|\mathbf{B}_h \nabla_{\Gamma_h} u_h\|_{L_2(T)}) \\ + h_T \|R - R_T\|_{L_2(T)}].$$

Next we bound the edge residual $\|[\nabla_{\Gamma_h} u_h]\|_{L_2(\partial T)}$. Let e be an edge which is shared by elements $T_1 = T$ and T_2 and whose closure contains the nodes z_1 and z_2 . Let $\lambda_{i,j}$, $i, j = 1, 2$, be the barycentric coordinate on triangle i corresponding to the vertex z_j , and define $\phi_e|_{T_i} = \lambda_{i,1}\lambda_{i,2}$. Thus $\phi_e \in H_0^1(T_1 \cup T_2)$, and $\phi_e > 0$ on e . Then

$$(3.3.28) \quad \|[\nabla_{\Gamma_h} u_h]\|_{L_2(e)} \leq C \|\sqrt{\phi_e} [\nabla_{\Gamma_h} u_h]\|_{L_2(e)}.$$

Noting that $[[\nabla_{\Gamma_h} u_h]]_e$ is a constant, we employ (3.3.5) with $\psi = ([\nabla_{\Gamma_h} u_h])_e \phi_e^\ell$ to find

$$(3.3.29) \quad \begin{aligned} \int_e |[\nabla_{\Gamma_h} u_h]|^2 \phi_e \, ds &= \int_{\tilde{T}_1 \cup \tilde{T}_2} \nabla_{\Gamma}(u - u_h^\ell) \nabla_{\Gamma}([[\nabla_{\Gamma_h} u_h]]_e \phi_e^\ell) \, d\sigma \\ &\quad - \int_{T_1 \cup T_2} R|[\nabla_{\Gamma_h} u_h]|_e \phi_e \, d\sigma_h + \int_{\tilde{T}_1 \cup \tilde{T}_2} [\mathbf{I} - \mathbf{A}_h^\ell] \nabla_{\Gamma} u_h^\ell \nabla_{\Gamma}([[\nabla_{\Gamma_h} u_h]]_e \phi_e) \, d\sigma \\ &\leq |[\nabla_{\Gamma_h} u_h]|_e (\|\nabla_{\Gamma}(u - u_h^\ell)\|_{L_2(\tilde{T}_1 \cup \tilde{T}_2)} \|\mathbf{A}_h\|_{L_\infty(T_1 \cup T_2)}^{1/2} \|\nabla_{\Gamma_h} \phi_e\|_{L_2(T_1 \cup T_2)} \\ &\quad + \|R\|_{L_2(T_1 \cup T_2)} \|\phi_e\|_{L_2(T_1 \cup T_2)} \\ &\quad + \|\mathbf{B}_h \nabla_{\Gamma_h} u_h\|_{L_2(T_1 \cup T_2)} \|\mathbf{A}_h\|_{L_\infty(T_1 \cup T_2)}^{1/2} \|\nabla_{\Gamma_h} \phi_e\|_{L_2(T_1 \cup T_2)}). \end{aligned}$$

A simple scaling argument yields $\|\phi_e\|_{L_2(T_1 \cup T_2)} \leq Ch_T$ and $\|\nabla_{\Gamma_h} \phi_e\|_{L_2(T_1 \cup T_2)} \leq C$, so that

$$(3.3.30) \quad \begin{aligned} \int_e |[\nabla_{\Gamma_h} u_h]|^2 \phi_e \, ds &\leq Ch_T^{-1/2} \|[\nabla_{\Gamma_h} u_h]\|_{L_2(e)} \\ &\quad \cdot [\|\mathbf{A}_h\|_{L_\infty(T_1 \cup T_2)}^{1/2} \|\nabla_{\Gamma}(u - u_h^\ell)\|_{L_2(\tilde{T}_1 \cup \tilde{T}_2)} \\ &\quad + h_T \|R\|_{L_2(T_1 \cup T_2)} + \|\mathbf{A}_h\|_{L_\infty(T_1 \cup T_2)}^{1/2} \|\mathbf{B}_h \nabla_{\Gamma_h} u_h\|_{L_2(T_1 \cup T_2)}]. \end{aligned}$$

Combining the previous three inequalities, we find that

$$(3.3.31) \quad \begin{aligned} h_T^{1/2} \|[\nabla_{\Gamma_h} u_h]\|_{L_2(e)} &\leq C (\|\mathbf{A}_h\|_{L_\infty(T_1 \cup T_2)}^{1/2} \|\nabla_{\Gamma}(u - u_h^\ell)\|_{L_2(\tilde{T}_1 \cup \tilde{T}_2)} \\ &\quad + h_T \|R\|_{L_2(T_1 \cup T_2)} + \|\mathbf{A}_h\|_{L_\infty(T_1 \cup T_2)}^{1/2} \|\mathbf{B}_h \nabla_{\Gamma_h} u_h\|_{L_2(T_1 \cup T_2)}). \end{aligned}$$

Summing (3.3.31) over the three edges of T and combining (3.3.31) with (3.3.27) completes the proof of (3.3.21). \square

4. Implementation details. In this section we provide some details concerning implementation.

4.1. Computation of geometric quantities. We assume that $\Gamma = \{x \in \mathbb{R}^3 : \zeta(x) = 0\}$, where ζ is sufficiently smooth with a nonzero gradient in a large enough neighborhood of Γ . In addition, we assume that ζ , its gradient, and its Hessian matrix are available and that for $x \in U$ we can approximate $a(x)$ with sufficient accuracy. In the next subsection we describe a simple approach for approximating $a(x)$.

First we note that if $x \in \Gamma$, $\vec{\nu}(x) = \frac{\nabla \zeta}{|\nabla \zeta|}$. Thus for $x \in U$,

$$(4.4.1) \quad \vec{\nu}(x) = \frac{\nabla \zeta(a(x))}{|\nabla \zeta(a(x))|}.$$

In addition, we have for $x \in \Gamma$

$$(4.4.2) \quad \mathbf{H}(x) = \nabla_{\Gamma} \vec{\nu}(x) = \mathbf{P} \nabla \frac{\nabla \zeta(x)}{|\nabla \zeta(x)|}.$$

For the sake of concreteness, we note that $\nabla \frac{\nabla \zeta(x)}{|\nabla \zeta(x)|}$ is not necessarily symmetric and that $[\nabla \frac{\nabla \zeta}{|\nabla \zeta|}]_{ij} = \frac{\partial}{\partial x_i} \frac{\zeta_{x_j}}{|\nabla \zeta|}$. The eigenvalues κ_1 and κ_2 of H in the directions orthogonal to $\vec{\nu}$ may then be approximated numerically. We also recall the relationship $\kappa_i(x) = \frac{\kappa_i(a(x))}{1+d(x)\kappa_i(a(x))}$ from (2.2.5). Finally, we emphasize that d is the *signed* distance function, that is, $d(x) = \text{sign}(\zeta(x))|a(x) - x|$ for $x \in U \setminus \Gamma$.

The above information is sufficient to implement the adaptive method described above. In particular, for $x \in \Gamma_h$ we use (2.2.23) to define the discrete data

$$(4.4.3) \quad f_h(x) = \mu_h(x)f(a(x)) = (1 - d(x)\kappa_1(x))(1 - d(x)\kappa_2(x))\vec{\nu}(x) \cdot \vec{\nu}_h(x)f(a(x)).$$

Here $\vec{\nu}(x)$ is computed via (4.4.1), κ_1 and κ_2 are computed via (2.2.5), and $\vec{\nu}_h$ must be computed from mesh information. Next we note that

$$(4.4.4) \quad \|\mathbf{A}_h(x)\|_{\ell_2 \rightarrow \ell_2} \leq \frac{\max(1 - d(x)\kappa_1(x), 1 - d(x)\kappa_2(x))}{|\vec{\nu}(x) \cdot \vec{\nu}_h(x)| \min(1 - d(x)\kappa_1(x), 1 - d(x)\kappa_2(x))} \equiv \bar{A}_h(x)$$

and

$$(4.4.5) \quad \begin{aligned} \|\mathbf{B}_h(x)\|_{\ell_2 \rightarrow \ell_2} &\leq \frac{1}{\mu_h(x)} [|d(x)(\kappa_1(x) - \kappa_2(x))| \\ &\quad + |1 - \vec{\nu}(x) \cdot \vec{\nu}_h(x)| (1 + 4 \max(1 - d(x)\kappa_1(x), 1 - d(x)\kappa_2(x)))] \\ &\equiv \bar{B}_h(x). \end{aligned}$$

The expressions on the right-hand sides of (4.4.4) and (4.4.5) may be computed using (4.4.1) and (2.2.5) as before. Since $\mathbf{P} - \mathbf{A}_h$ and \mathbf{B}_h are of higher order, using the above approximations for the norms of \mathbf{A}_h and \mathbf{B}_h should lead to at most a slight overestimation of the overall error while yielding nontrivial computational savings.

4.2. Computation of d and a . The efficient computation of the projection a and distance function d are central to implementing the finite element method and a posteriori estimators described here. In a very few cases, d is available explicitly (for example, $d(x) = |x| - r$ for a sphere of radius r). Even for relatively simple surfaces such as ellipsoids, however, an explicit expression for d is not available and a and d must be approximated. Since d is assumed to be smooth and we need to be concerned only about starting points sufficiently close to Γ , standard methods of nonlinear optimization are, in principle, applicable.

We have tested two different algorithms for computing a : one being Newton's method and the other being an ad hoc first-order method. Before describing the methods we note a relationship which we shall use in our algorithms. For $x \in U$, $\zeta(x) = \int_0^{d(x)} \nabla \zeta(a(x) + t\vec{\nu}(x)) \cdot \vec{\nu}(x) dt = d|\nabla \zeta(x)| + O(d^2)$. Thus

$$(4.4.6) \quad d(x) \approx \frac{\zeta(x)}{|\nabla \zeta(x)|}.$$

Next we describe our implementation of Newton's method. Assume that $x_0 \in U$ and that we wish to compute $a(x_0)$. In order to employ Newton's method, we seek a stationary point of the function $F(x, \lambda) = |x - x_0| + \lambda \zeta(x)$. Note that $\nabla F(x, \lambda) = (2(x - x_0) + \lambda \nabla \zeta(x), \zeta(x))$. Thus $\nabla F(x, \lambda) = 0$ implies that $x \in \Gamma$ and $(x - x_0)$ is parallel to $\nabla \zeta(x)$, that is, $x = a(x_0)$. In order to choose a starting point, we note that $2(x - x_0) + \lambda \nabla \zeta(x) = 0$ implies that $\lambda = 2d(x_0)/|\nabla \zeta(x)|$. Using (4.4.6), we thus choose the starting value $(x_0, \lambda_0) = (x_0, 2\phi(x_0)/|\nabla \phi(x_0)|^2)$ for Newton's method. Given a

tolerance tol , we iterate Newton's method until

$$(4.4.7) \quad \left(\frac{\zeta(x)^2}{|\nabla\zeta(x)|^2} + \left| \frac{\nabla\zeta(x)}{|\nabla\zeta(x)|} - \frac{x - x_0}{|x - x_0|} \right|^2 \right)^{1/2} < tol.$$

Fulfillment of this stopping criteria guarantees that the returned value $x \approx a(x_0)$ lies in the correct direction from x_0 to within tol and that, because of (4.4.6), $d(x) < tol$ up to higher-order terms.

The first-order algorithm which we employed may be described as follows: Since $a(x) = x - d(x)\vec{\nu}(x)$, we may use (4.4.6) and $\vec{\nu}(x) \approx \frac{\nabla\zeta(x)}{|\nabla\zeta(x)|}$ to approximate a by $a(x) \approx x - \frac{\zeta(x)\nabla\zeta(x)}{|\nabla\zeta(x)|^2}$. Iterating this relationship leads to an algorithm which converges to some point on Γ but not generally to $a(x)$. We thus correct the direction $x - x_0$ at each step, yielding the following algorithm.

1. Stipulate tol and x_0 , and initialize $x = x_0$.
2. While (4.4.7) is not satisfied, iterate the following steps:
 - (a) Calculate $\tilde{x} = x - \frac{\zeta(x)\nabla\zeta(x)}{|\nabla\zeta(x)|^2}$ and $dist = \text{sign}(\zeta(x_0))|\tilde{x} - x_0|$.
 - (b) Set $x = x_0 - dist \frac{\nabla\zeta(\tilde{x})}{|\nabla\zeta(\tilde{x})|}$.

In practice, the second of the two algorithms was more efficient than Newton's method. While Newton's method converged in less steps as one would expect, each step is relatively expensive. We also note that we have not rigorously analyzed the error in either of these methods which results from using the stopping criterion (4.4.7). A more rigorous analysis of robust algorithms for approximating a would thus be desirable.

5. Computational examples. In this section we describe several computational examples. All computations were performed using the finite element toolbox ALBERTA [SS05], and graphics were processed using the software GMV [Or05]. Also, the constant C appearing in the estimator Θ in (3.3.20) was taken to 0.25 in all calculations.

5.1. Example 1: Computation on a spherical subdomain. In our first test we consider a problem which was used as an example in the paper [AP05]. This problem demonstrates the ease with which our method handles problems in which the distance function is explicitly available and also provides a convenient place to consider surfaces with boundaries.

Let S^2 be the unit sphere with angular spherical coordinates (ϕ, θ) , where ϕ ($0 \leq \phi < 2\pi$) is the azimuthal angle in the xy -plane and $\theta = \cos^{-1} z$ ($0 \leq \theta \leq \pi$) is the polar angle from the z -axis. Following [AP05], we let Γ consist of points in S^2 such that $0 \leq \phi \leq \frac{5\pi}{3}$, and let $u(\phi, \theta) = (\sin \theta)^\lambda \sin \lambda \phi$ for $\lambda = .6$. Then u satisfies $-\Delta_\Gamma u = f$ in Γ and $u = 0$ on $\partial\Gamma$ with $f = \lambda(\lambda + 1)(\sin \theta)^\lambda \sin \lambda \phi$. Note that u is singular at the poles, so we may expect an adaptive algorithm to refine more heavily there.

Computation of the geometric quantities necessary to implement our method is quite straightforward. We employ the distance function $d(x) = |x| - 1$ for the sphere (note that we do not actually require access to the distance function for Γ here). In addition, we may easily compute that $\vec{\nu}(x) = \frac{x}{|x|}$, $a(x) = \frac{x}{|x|}$, and $\mathbf{H}_{ij}(x) = \frac{\delta_{ij}}{|x|} - \frac{x_i x_j}{|x|^3}$. The eigenvalues of $\mathbf{H}(x)$ are the principle curvatures of the sphere of radius $|x|$, that is, $\kappa_1 = \kappa_2 = \frac{1}{|x|}$. Computation of μ_h , \bar{A}_h , and \bar{B}_h is similarly straightforward.

In Figure 5.1, the initial mesh of six elements is displayed along with an adaptively refined mesh colored with the solution u_h . A blowup showing refinement near the

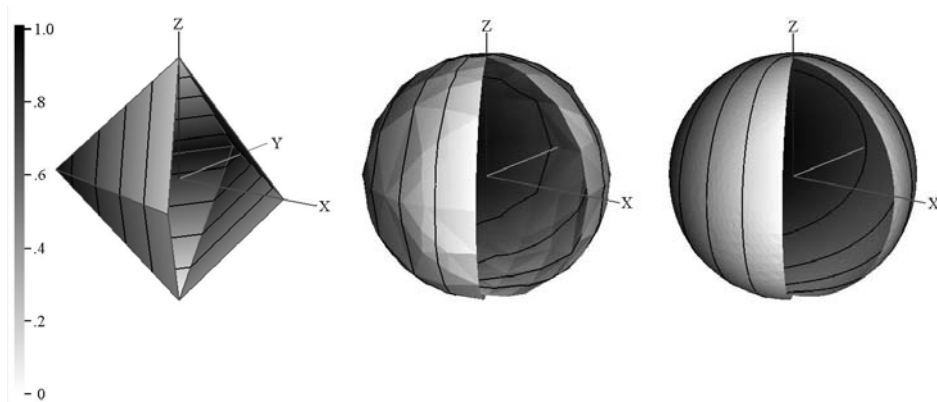


FIG. 5.1. *Experiment 1: The initial mesh with 6 nodes (left) and adaptively refined meshes with 151 (center) and 5559 (right) DOF displaying u_h .*

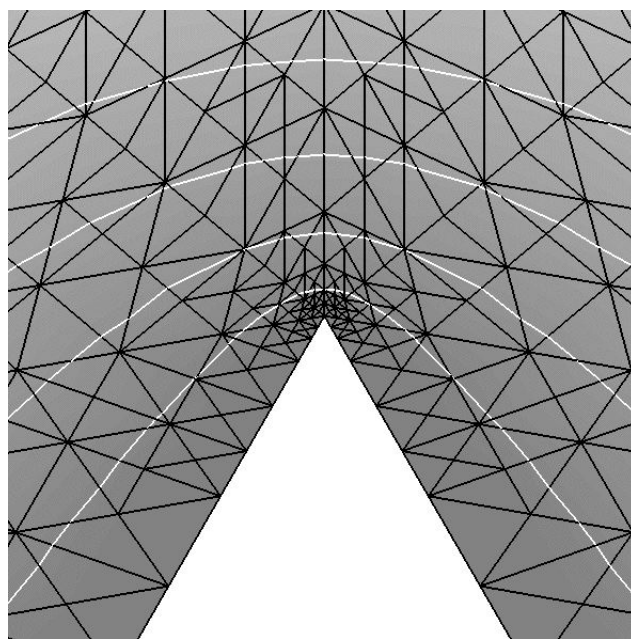


FIG. 5.2. *Experiment 1: View of the refined mesh along the z -axis, magnified $80\times$, with contour lines of u .*

positive z -pole is displayed in Figure 5.2. Finally, a graph displaying the error, the residual estimator Θ defined in (3.3.20), and various geometric quantities is given in Figure 5.3. First note that the quantity $\max_{T \in \mathcal{T}_h} h_T / \sqrt{|T|}$ appears to reach a maximum value of about 3. Thus our assumption in Corollary 3.2 that the mesh is shape-regular is justified for this example. Also, the error $\|\nabla_{\Gamma}(u - u_h^{\ell})\|_{L_2(\Omega)}$ and the residual estimator Θ converge with optimal order and appear to have a constant ratio as the mesh is refined. Finally, the quantities $\|\bar{B}_h|\nabla_{\Gamma_h} u_h|\|_{L_2(\Gamma_h)}$ and $\|1 - \bar{A}_h\|_{L_{\infty}(\Gamma_h)}$ are plotted and show second-order convergence, confirming experimentally our theoretical observation that these geometric contributions to the error are of

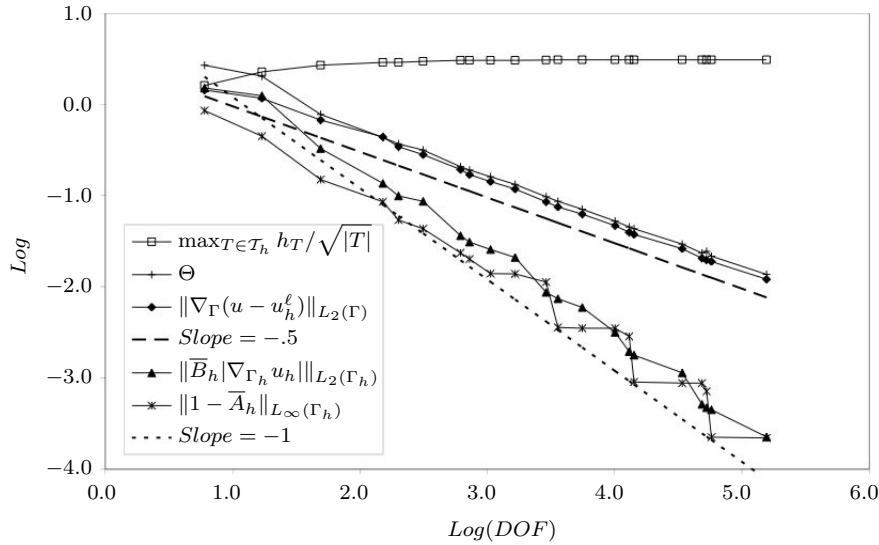


FIG. 5.3. Experiment 1: Error, estimator, and various geometric quantities.

higher order. It is worth noting here that the quantity \bar{A}_h appears in the estimator as a multiplicative factor. Since it converges to 1, it would thus be reasonable and computationally more efficient to omit it entirely once $\|\bar{A}_h\|_{L^\infty(\Gamma_h)}$ is observed to reach a given tolerance.

5.2. Example 2: Computation on a torus. In our second test we performed a computation on a torus. $d(x) = \sqrt{(r_0 - \sqrt{x^2 + y^2})^2 + z^2} - r_1$ is the signed distance function for a torus whose axis of revolution is the z -axis, whose radius of revolution is r_0 , and which has thickness $2r_1$. The other necessary geometric quantities may be computed from this formula. We took $r_0 = 1$ and $r_0 = 0.25$. As a test solution we took the function

$$(5.5.1) \quad u(x, y, z) = e^{\frac{1}{1.85-x^2}} \sin y,$$

which has exponential peaks on the outer portions of the torus which lie near the x -axis.

In Figure 5.4 we display \bar{A}_h on the the initial 24-node mesh; note that here \bar{A}_h is about 5 on the outer edge of the torus, so it enters into the calculation in a significant way. Also displayed in Figure 5.4 is a refined mesh having 1248 nodes and displaying the discrete solution u_h . In Figure 5.5 we display the local H_1 error contributions along with the three components \bar{A}_h , η_T , and $\bar{B}_h|\nabla_{\Gamma_h} u_h|$ of the estimator Θ . The local residual indicator η_T reflects reasonably well the local error distribution, while the contributions from \bar{A}_h and $\bar{B}_h|\nabla_{\Gamma_h} u_h|$ are relatively insignificant. Also, the maximum ratio $h_T/\sqrt{|T|}$ observed during this calculation was 5.28. This relatively large number reflects the fact that the triangles in the initial mesh displayed in Figure 5.4 already have relatively high aspect ratios.

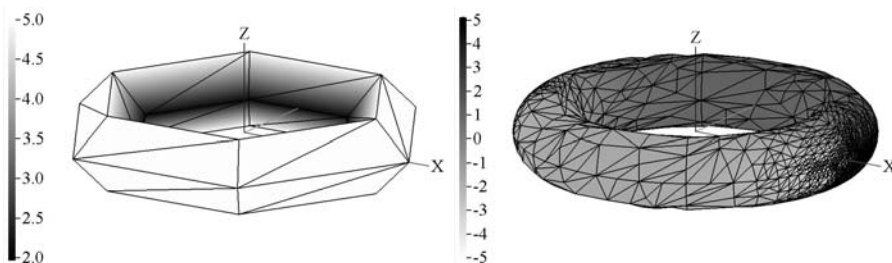


FIG. 5.4. *Experiment 2: The initial mesh displaying \bar{A}_h (left) and the refined mesh with 1248 DOF displaying u_h (right).*

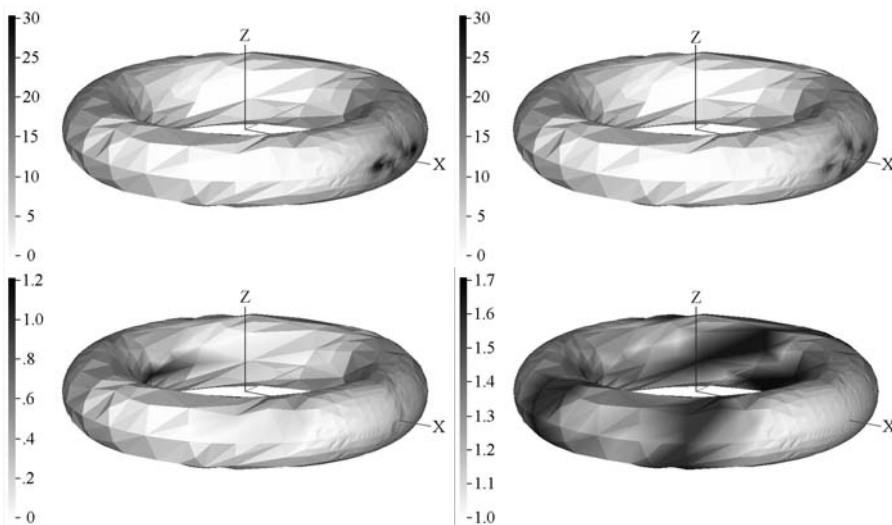


FIG. 5.5. *Experiment 2: The local residual η_T (top left), H_1 error (top right), $\bar{B}_h |\nabla_{\Gamma_h} u_h|$ (bottom left), and \bar{A}_h (bottom right).*

5.3. Example 3: Computation on an ellipsoid. In our third computational example we let Γ be an ellipsoid satisfying the level set equation

$$(5.5.2) \quad x^2 + y^2 + \frac{z^2}{400} = 1.$$

As a test solution we took $u(x, y, z) = \sin y$ so that u and its derivatives were of moderate size.

In Figure 5.6 we display the local residual contribution η_T and the local geometric error $\bar{B}_h |\nabla_{\Gamma_h} u_h|$ on an adaptively refined mesh having 10383 nodes. Note that the maximum values of η_T and $\bar{B}_h |\nabla_{\Gamma_h} u_h|$ are approximately equal. Thus the geometric error plays a role in the marking of some elements even on a refined mesh. As in Figure 5.3, however, the overall geometric error $\|\bar{B}_h |\nabla_{\Gamma_h} u_h|\|_{L_2(\Gamma_h)}$ declines approximately as DOF^{-1} , while the residual error $(\sum_{T \in \mathcal{T}_h} \eta_T^2)^{1/2}$ declines as $\text{DOF}^{-1/2}$ (we do not display a chart for the current situation as it is entirely analogous to Figure 5.3). Finally, the maximum ratio $h_T / \sqrt{|T|}$ observed in this adaptive calculation (up 64521 DOF) was 3.41, so that mesh quality remained reasonable.

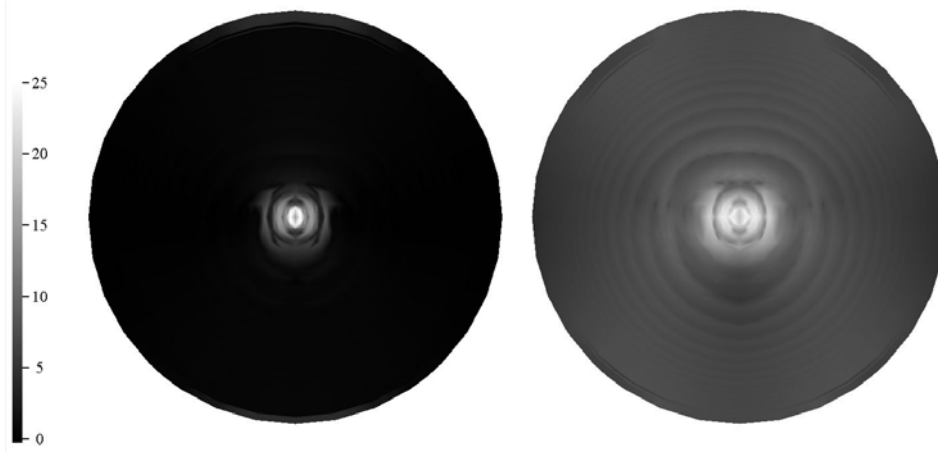


FIG. 5.6. Experiment 3: Mesh with 10383 nodes displaying the relative sizes of $\bar{B}_h |\nabla_{\Gamma_h} u_h|$ (left) and the local residual η_T (right). The view is along the z -axis.

Appendix. Proof of Proposition 2.1. Proposition 2.1 is potentially of interest in other situations (e.g., when Γ_h is a higher-order polynomial approximation to Γ), so we begin by stating a more general version.

PROPOSITION A.1. Let \hat{T} be the unit simplex in \mathbb{R}^2 , and suppose that $F : \hat{T} \rightarrow U$ is a C^1 mapping whose gradient has two nonzero singular values at each point in \hat{T} . Suppose $x \in T := F(\hat{T})$, let \vec{v}_h be the normal to T at x , and let $d\sigma_h$ be a surface measure on T . Assume also that $\vec{v} \cdot \vec{v}_h > 0$. Letting $d\sigma_h(x)\mu_h(x) = d\sigma(x)$, we then have

$$(A.A.1) \quad \mu_h(x) = \vec{v} \cdot \vec{v}_h (1 - d(x)\kappa_1(x))(1 - d(x)\kappa_2(x)).$$

Proof. We fix a point $\hat{x} \in \hat{T}$ and let $x = F(\hat{x})$ and $\mathbb{R}^{3 \times 2} \ni \mathbf{A} = \nabla F(\hat{x})$. Let $\{\vec{e}_1, \vec{e}_2\}$, $\{\vec{u}_1, \vec{u}_2\}$, and $\{\vec{v}_1, \vec{v}_2\}$ be orthonormal bases for \mathbb{R}^2 and the tangent spaces to Γ_h and Γ at x and $a(x)$, respectively. We assume also that $\{\vec{v}_1, \vec{v}_2, \vec{v}\}$ are the eigenvectors of $(\mathbf{I} - d\mathbf{H})(x)$ corresponding to the eigenvalues $\lambda_1 = 1 - d(x)\kappa_1(x)$, $\lambda_2 = 1 - d(x)\kappa_2(x)$, and $\lambda_3 = 1$. Letting \times denote the cross product, we have $d\sigma_h = |\mathbf{A}\vec{e}_1 \times \mathbf{A}\vec{e}_2| d\hat{x}$ and $d\sigma = |(\mathbf{I} - d\mathbf{H})[\mathbf{P}][\mathbf{A}]\vec{e}_1 \times (\mathbf{I} - d\mathbf{H})[\mathbf{P}][\mathbf{A}]\vec{e}_2| d\hat{x}$.

Next we recall the formula $(\mathbf{B}\vec{x}_1) \times (\mathbf{B}\vec{x}_2) = \mathbf{B}_{adj}(\vec{x}_1 \times \vec{x}_2)$, where \mathbf{B} is symmetric and nonsingular and $\mathbf{B}_{adj} = (\det \mathbf{B})\mathbf{B}^{-1}$. Noting that $(\mathbf{I} - d\mathbf{H})_{adj}$ has eigenvectors $\{\vec{v}_1, \vec{v}_2, \vec{v}\}$ with eigenvalues $\{\lambda_2\lambda_3, \lambda_1\lambda_3, \lambda_1\lambda_2\}$, we calculate

$$(A.A.2) \quad \begin{aligned} & (\mathbf{I} - d\mathbf{H})[\mathbf{P}][\mathbf{A}]\vec{e}_1 \times (\mathbf{I} - d\mathbf{H})[\mathbf{P}][\mathbf{A}]\vec{e}_2 = \lambda_2\lambda_3[(\mathbf{P}[\mathbf{A}]\vec{e}_1 \times \mathbf{P}[\mathbf{A}]\vec{e}_2) \cdot \vec{v}_1]\vec{v}_1 \\ & + \lambda_1\lambda_3[(\mathbf{P}[\mathbf{A}]\vec{e}_1 \times \mathbf{P}[\mathbf{A}]\vec{e}_2) \cdot \vec{v}_2]\vec{v}_2 + \lambda_1\lambda_2[(\mathbf{P}[\mathbf{A}]\vec{e}_1 \times \mathbf{P}[\mathbf{A}]\vec{e}_2) \cdot \vec{v}]\vec{v}. \end{aligned}$$

But $(\mathbf{P}[\mathbf{A}]\vec{e}_1 \times \mathbf{P}[\mathbf{A}]\vec{e}_2) \perp \vec{v}_i$, $i = 1, 2$, $(\mathbf{P}[\mathbf{A}]\vec{e}_1 \times \mathbf{P}[\mathbf{A}]\vec{e}_2) \cdot \vec{v} = (\mathbf{A}\vec{e}_1 \times \mathbf{A}\vec{e}_2) \cdot \vec{v}$, and $\mathbf{A}\vec{e}_1 \times \mathbf{A}\vec{e}_2 \parallel \vec{v}_h$. Thus

$$(A.A.3) \quad \begin{aligned} d\sigma &= |(\mathbf{I} - d\mathbf{H})[\mathbf{P}][\mathbf{A}]\vec{e}_1 \times (\mathbf{I} - d\mathbf{H})[\mathbf{P}][\mathbf{A}]\vec{e}_2| d\hat{x} \\ &= \lambda_1\lambda_2[(\mathbf{A}\vec{e}_1 \times \mathbf{A}\vec{e}_2) \cdot \vec{v}]\vec{v} d\hat{x} = \lambda_1\lambda_2|\mathbf{A}\vec{e}_1 \times \mathbf{A}\vec{e}_2|\vec{v}_h \cdot \vec{v} d\hat{x}. \end{aligned}$$

Recalling that $d\sigma_h = |\mathbf{A}\vec{e}_1 \times \mathbf{A}\vec{e}_2| d\hat{x}$ completes the proof. \square

REFERENCES

- [AO00] M. AINSWORTH AND J. T. ODEN, *A Posteriori Error Estimation in Finite Element Analysis*, Pure Appl. Math. (NY), Wiley-Intersci. Hoboken, NJ, 2000.
- [AP05] T. APEL AND C. PESTER, *Clement-type interpolation on spherical domains—interpolation error estimates and application to a posteriori error estimation*, IMA J. Numer. Anal., 25 (2005), pp. 310–336.
- [BMN05] E. BÄNSCH, P. MORIN, AND R. H. NOCHETTO, *A finite element method for surface diffusion: The parametric case*, J. Comput. Phys., 203 (2005), pp. 321–343.
- [BCD04] S. BARTELS, C. CARSTENSEN, AND G. DOLZMANN, *Inhomogeneous Dirichlet conditions in a priori and a posteriori finite element error analysis*, Numer. Math., 99 (2004), pp. 1–24.
- [CDDRR04] U. CLARENZ, U. DIEWALD, G. DZIUK, M. RUMPF, AND R. RUSU, *A finite element method for surface restoration with smooth boundary conditions*, Comput. Aided Geom. Design, 21 (2004), pp. 427–445.
- [DR98] W. DÖRFLER AND M. RUMPF, *An adaptive strategy for elliptic problems including a posteriori controlled boundary approximation*, Math. Comp., 67 (1998), pp. 1361–1382.
- [DW00] W. DÖRFLER AND O. WILDEROTTER, *An adaptive finite element method for a linear elliptic equation with variable coefficients*, ZAMM Z. Angew. Math. Mech., 80 (2000), pp. 481–491.
- [Dz88] G. DZIUK, *Finite elements for the Beltrami operator on arbitrary surfaces*, in Partial Differential Equations and Calculus of Variations, Lecture Notes in Math. 1357, Springer, Berlin, 1988, pp. 142–155.
- [Dz91] G. DZIUK, *An algorithm for evolutionary surfaces*, Numer. Math., 58 (1991), pp. 603–611.
- [FV06] F. FIERRO AND A. VEESER, *A posteriori error estimates, gradient recovery by averaging, and superconvergence*, Numer. Math., 103 (2006), pp. 267–298.
- [GT98] D. GILBARG AND N. S. TRUDINGER, *Elliptic Partial Differential Equations of Second Order*, 2nd ed., Springer, Berlin, 1998.
- [Ho01] M. HOLST, *Adaptive numerical treatment of elliptic systems on manifolds*, Adv. Comput. Math., 15 (2001), pp. 139–191.
- [MN05] K. MEKCHAY AND R. H. NOCHETTO, *Convergence of adaptive finite element methods for general second order linear elliptic PDEs*, SIAM J. Numer. Anal., 43 (2005), pp. 1803–1827.
- [MNS02] P. MORIN, R. H. NOCHETTO, AND K. G. SIEBERT, *Convergence of adaptive finite element methods*, SIAM Rev., 44 (2002), pp. 631–658. Revised reprint of *Data oscillation and convergence of adaptive FEM*, SIAM J. Numer. Anal., 38 (2000), pp. 466–488.
- [Or05] F. A. ORTEGA, *GMV Version 3.8*, Technical rep. LA-UR-95-2986, Los Alamos National Laboratory, Los Alamos, NM, 2005.
- [SS05] A. SCHMIDT AND K. G. SIEBERT, *Design of adaptive finite element software*, in The Finite Element Toolbox ALBERTA, Lec. Notes Comput. Sci. Eng. 42, CD-ROM, Springer, Berlin, 2005.
- [Ver89] R. VERFÜRTH, *A posteriori error estimators for the Stokes equations*, Numer. Math., 55 (1989), pp. 309–325.